Proceedings of 2018 IEEE
International Conference on Mechatronics and Automation
August 5 - 8, Changchun, China

Weld Seam Type Recognition System Based on Structured Light Vision and Ensemble Learning

Zhe Wang[1,2]
[1]*Institute of Automation, Chinese Academy of Sciences*
[2]*University of Chinese Academy of Sciences*
Beijing, China
wangzhe2016@ia.ac.cn

Fengshui Jing[1,2] and Junfeng Fan[1,2]
[1]*Institute of Automation, Chinese Academy of Sciences*
[2]*University of Chinese Academy of Sciences*
Beijing, China
{fengshui.jing & fanjunfeng2014}@ia.ac.cn

***Abstract* - In this paper, we propose a weld seam recognition system based on structured light vision and ensemble learning. The proposed system consists of an industrial robot, a structured light vision sensor and a computer. The recognition procedures of proposed system include weld seam feature extraction and weld seam classification. In feature extraction part, the input images are processed by the following steps: noise filtration, laser stripe pattern extraction, main line extraction, edge points detection and feature computation. In classification part, ensemble learning models including BP-Adaboost and KNN-Adaboost are established to classify the images by the feature extracted. The experiment results validate the effectiveness and robustness of the proposed recognition system.**

Index Terms - weld seam type recognition, feature extraction, structured light vision, ensemble learning algorithm.

I. Introduction

Nowadays, with the trend of intelligent manufacturing, automatic and robotic welding is becoming increasingly popular in welding industry. However, full-automatic robotic welding system is yet to be effectively actualized. This is because the quality of automatic welding process is affected by factors including the disturbance from welding arc lights and splashes, the variety of weld seam structure, the weld seam distortion caused by welding heat and so on [1].

In order to solve these problems, one of the most important procedures is to precisely acquire the structure information of the weld seam using sensors. At present, different kinds of sensors have been applied in robotic welding, such as arc sensors [2], ultrasonic sensors [3], acoustic sensors [4] and vision sensors [5-7]. Among them, vision sensors are widely applied in welding process with the advantages of high precision and non-contact quality. Particularly, in arc welding environment with optical disturbance, structured light vision sensor is considered a practical sensor due to its high accuracy, excellent real-time and anti-interference ability [8].

The structured-light images of different welding seam types are distinguishing from each other. Meanwhile, in robotic welding, the selection of welding voltage, current, speed and other parameters is closely related to the welding seam type. Nevertheless, most of the vision systems in welding application cannot automatically recognize weld seam types and require manual input, which lowers the efficiency and adaptability. Recently, some researchers have been studying on the automatic recognition of weld seam type based on structured-light. Wang et al. [9] proposed a recognition method based on wavelet transform and probabilistic neural network. However, the design of weld seam features does not have the property of multi-scale invariance, thus lowers the adaptability. Fan et al. [10] proposed a weld seam type recognition system based on SVM classifier, which achieves the recognition with low computation cost. Nevertheless, SVM is a binary classifier [11], which would make the model complex in multi-classification tasks. Therefore, it is necessary to develop a welding seam recognition method with ideal accuracy, efficiency and adaptability.

Ensemble learning algorithm is a widely used algorithm for classification and prediction, which combines multiple machine learning algorithms to obtain better performance. The ensemble model has much stronger generalization ability and higher accuracy than the member learners [12]. Thus, ensemble learning algorithm is chosen as the classification algorithm in proposed system.

In this paper, a weld seam recognition system based on structured light vision and ensemble learning is proposed. The proposed system possesses three properties. Firstly, the noises from the welding arc lights can be filtered out by multi-frame processing and specialized image filters. Secondly, a novel method of laser stripe and feature point extraction is proposed to precisely compute the feature vectors. Thirdly, ensemble learning algorithm based on Adaboost algorithm is adopted to solve the multi-classification problem. Therefore, with the proposed system, the weld seam type can be precisely and efficiently recognized in various working condition. Thus, the welding parameters can be automatically selected according to the weld seam type in the following welding procedures.

In the remainder of this paper, the experiment system is presented in Section II. The image processing and feature extraction process is presented in Section III. Section IV presents the classification model and Section V presents the experiment results. Finally, the paper is concluded in Section VI.

II. Experiment System

There proposed recognition system consists of robotic system, vision sensor and computer. The robotic system is industrial robot MOTOMAN and its controller made by

* This research was supported by the National Natural Science Foundation of China under Grant No.61573358.

978-1-5386-6075-1/18/$31.00 ©2018 IEEE

YASKAWA Corporation. It is adopted to mount the welding torch and the vision sensor and to move along the weld seam. The vision sensor device is composed of a CCD camera, a stripe laser emitter, and an optical filter. The 635-nm laser emitter serves as structured light source to project laser stripe onto the weld seam. The optical filter is a narrow band filter whose band centered at 635 nm, the same as the laser wavelength to filter out arc light noises. It is placed in front of the lens of CCD camera. The camera captures the structure-light images on the weld seam. The computer is used to run the image processing and weld seam type recognition algorithm while serving as the interface of the system.

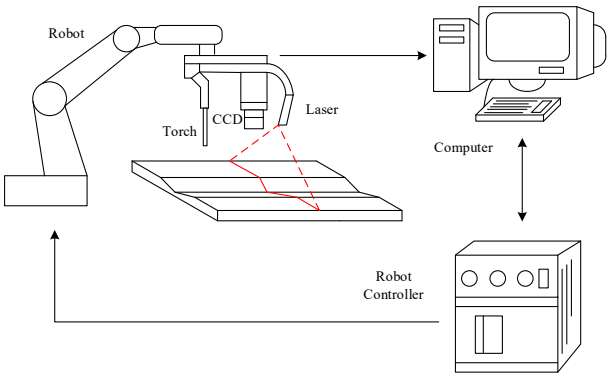

Fig. 1 Schematic diagram of proposed system.

III. Weld Seam Feature Extraction

According to the groove form, welding seam types can be divided into six categories, including symmetric V groove, left side V groove, right side V groove, left lap joint groove, right lap joint groove and square groove. The structured light images (without noises) of different weld seam types are as shown in Fig.2. It is shown that the laser stripe includes several pieces of linear segments. The shape of laser stripe on the welding joint is distinct among different types of weld seams. Hence it can be extracted as weld seam feature for recognition. In addition, it is shown that the laser stripe in Fig.2 is several pixels in width and is straight on the surface of the work piece. These characteristics can be utilized in order to extract weld seam feature precisely.

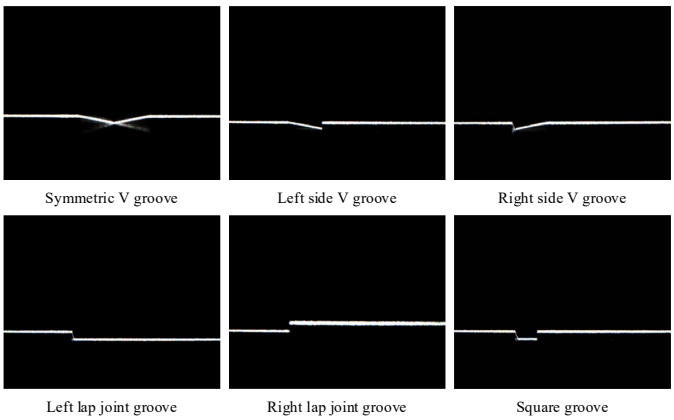

Fig. 2 Structured light images of different weld seam types.

A. Image Pre-processing

1) Multiple Frame Processing: In general, the laser stripe pattern in structured-light images during welding process could be polluted by noises from welding arc lights and splashes. Our proposed experiment system utilizes a narrow band optical filter to filter out noises from arc lights. However, the splashes still remain in the images. In the image sequence captured from the camera, it is found that splashes are generally instantaneous while the laser stripe pattern is stable between consecutive frames. Therefore, multiple frame processing is adopted to filter out splashes. In this operation, the smallest intensity of corresponding pixels is taken between consecutive frames. The result of multiple frame processing between two consecutive frames Fig.3a and Fig.3b is shown in Fig.3c. It is shown that most splash noises are eliminated.

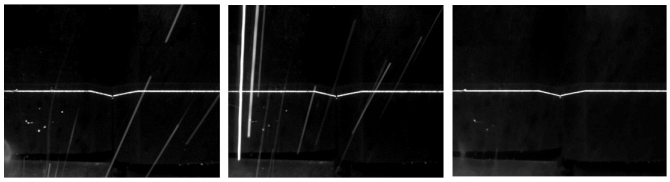

Fig. 3 The process of multiple frame processing.

2) Morphological Filter: In mathematical morphology, a structuring element is used for probing the input image. The effect of opening filter and closing filter is closely related to the property of structuring element.

As is shown in Fig.3c, there are some minor noises (small groups of bright pixels) still remaining in the image which need to be filtered out. Since the noises are small in area, morphological opening filter with a relatively small-sized structuring element was used to eliminate these noises. However, due to the unevenness of the surface, there are gaps and holes (groups of dark pixels) in the laser stripe pattern. The opening filter may enlarge the gaps to some extent. Therefore, morphological closing filter with a relatively large-sized structuring element was used to fill the gaps and holes and make the stripe pattern continuous.

3) Modified Anisotropy Diffusion Filter: Anisotropy diffusion filter based on partial differential equation can filter out image noise without blurring edges. The region boundaries in the image remain sharp after the filtration process [13]. This characteristic makes it capable of smoothening the burrs on the laser stripe without removing the edges that are important for the interpretation of the laser stripe pattern. The diffusion model is described as follows:

$$I^{t+1} = I^t + \lambda \sum_d c_d \nabla f_d(I^t) \ , \ d = \{U, D, L, R\} \qquad (1)$$

where I^t and I^{t+1} is the gray value of pixel point before and after diffusion process, λ is the parameter that controls the intensity of the operation, d is the direction of diffusion, *U, D, L,* and *R* are the abbreviations for up, down, left and right respectively, the symbol ∇f_d indicates nearest-neighbor differ-

ences and c_d is conduction coefficient that is computed with (2)

$$c_d = e^{-|\nabla f_d(I)|^2/k^2} \quad , \ d = \{U, D, L, R\} . \tag{2}$$

where k is diffusion coefficient that controls the efficient of conduction.

The traditional anisotropy diffusion filter calculates the ∇f_d value of a pixel using the its difference with its nearest neighbor. However, its performance declines where there are high intensity salt-and-pepper noises and burrs with high gray value. When the nearest-neighbor differences brought by high intensity noises exceed the differences between edges and the background, the noises would remain in the image after the filtration. In the structured-light image, it is notable that the gray value of every pixel in the laser stripe pattern is much higher than the background, and the stripe pattern is several pixels in width. Based on this fact, a modified computation of ∇f_d that uses three neighboring pixels to calculate the difference enables the operation to filter out high intensity salt-and-pepper noises and burrs. Thus, the value of ∇f_d is computed as follows:

$$\nabla f_U(I_{x,y}) = \alpha I_{x,y-2} + (1-\alpha) I_{x,y-1} - I_{x,y} \tag{3}$$

$$\nabla f_D(I_{x,y}) = \alpha I_{x,y+2} + (1-\alpha) I_{x,y+1} - I_{x,y} \tag{4}$$

$$\nabla f_L(I_{x,y}) = \alpha I_{x-2,y} + (1-\alpha) I_{x-1,y} - I_{x,y} \tag{5}$$

$$\nabla f_R(I_{x,y}) = \alpha I_{x+2,y} + (1-\alpha) I_{x+1,y} - I_{x,y} \tag{6}$$

where the direction w is up, down, left and right respectively, α is the weight coefficient and $0<\alpha<0.5$.

B. Laser Stripe Pattern Extraction

1) Region of Interest Determination: The determination of region of interest(ROI) could not only reduce the computational cost but also improve feature extraction precision in further steps of image processing. The region that includes laser stripe segments on the welding joint from where the features are extracted is chosen as ROI in this image. Since the laser stripe pattern is approximately parallel with x axis of the image, by projecting the gray value of each row onto y axis, the approximate y position of the laser stripe is determined by row index of the peak value. The projection operation is as follows:

$$P_v(i) = \sum_{j=1}^{w} I(i,j) \ , \ i = 1, 2, ..., h \tag{7}$$

where $P_v(i)$ is sum of gray value of the i-th row, $I(i, j)$ is the gray value of pixel point (i, j), and h and w are the height and width of the image respectively. The result of projection is shown in Fig.4. From the figure, it is shown that there is a distinct peak in the projection result. Therefore, the ROI is determined around the peak area. The computation of ROI is as follows:

$$[y_{\min}, y_{\max}] = [\arg\max_i P_v(i) - \Delta y, \arg\max_i P_v(i) + \Delta y] \tag{8}$$

where $[y_{\min}, y_{\max}]$ is the boundary of ROI in y axis, Δy is the range from center of ROI to the boundary in y axis.

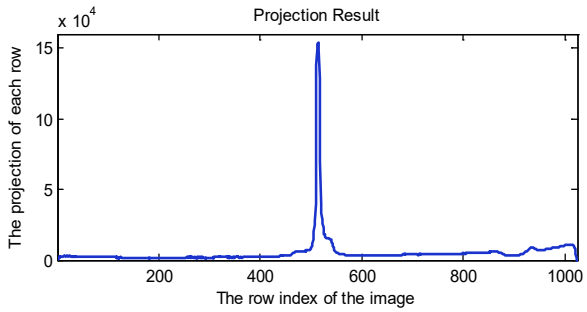

Fig. 4 The gray value projection result.

2) Extraction of Center Profile: After the filtration process, the upper and lower edges of the laser stripe are smooth. Thus, the center profile can be extracted by averaging the location of upper and lower edges. The edges are detected using derivatives of neighboring gray value of each row. The computation is as follows:

$$E_a(j) = \arg\max_k G_a(k) \quad (j = 1, 2, ..., w) \tag{9}$$

$$G_a(k) = \sum_{i=k}^{k+1} \beta_{i-k+1} I(i,j) - \sum_{i=k-2}^{k-1} \beta_{k-i} I(i,j) \tag{10}$$

$$E_b(j) = \arg\min_k G_b(k) \quad (j = 1, 2, ..., w) \tag{11}$$

$$G_b(k) = \sum_{i=k+1}^{k+2} \beta_{i-k} I(i,j) - \sum_{i=k-1}^{k} \beta_{k-i+1} I(i,j) \tag{12}$$

$$\beta = [\beta_1, \beta_2] \ , \ \beta_1 > \beta_2 \tag{13}$$

where $E_a(j)$ and $E_b(j)$ are the upper and lower boundary point of the laser stripe in j-th column respectively, $G_a(k)$ and $G_b(k)$ are the derivative calculations of upper and lower edges in k-th point of j-th column respectively, w is the width of the image, and β is the weighting factor of pixels and the weight of the nearest pixel to the edge is larger. The result of upper and lower edges extraction is shown as the green line and red line in Fig.5a.

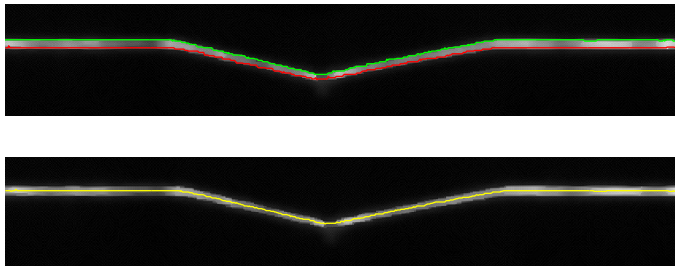

Fig. 5 Upper and lower edges extraction (a) and center profile extraction (b).

Then, the center profile of laser stripe is computed with sub-pixel precision as follows:

$$C(j) = \frac{1}{2}(E_a(j) + E_b(j)) \quad (j = 1, 2, ..., w) \tag{14}$$

where $C(j)$ is the center profile point in j-th column. The center profile extraction result of laser stripe is shown as the yellow line in Fig.5b.

C. Computation of Weld Seam Feature Vector

1) Main Line Extraction Based on Radon Transform: The main line is defined as the longest straight line segment of the laser stripe. It can be used as the benchmark when computing the feature of the stripe on the joint. Radon transform is applied on the center profile in order to extract the main line.

The Radon transform is the integral transform that projects the image intensity along a particular line and its value is the line integral of the image over that line. For the image of center profile, the radon transform is computed as follows:

$$R(L)=\int_L I(i,j)dl \tag{15}$$

where $R(L)$ is the corresponding integral value of straight line L. As is shown in (15), the more pixels the line passes through, the larger the $R(L)$ value is. If the image is converted into parameter space, straight line L can be represented as $[\rho,\theta]$ with ρ representing the distance to the center of the image and θ representing the angle between line L and the horizontal axis. Therefore, the integral value can be represented as $R(\rho,\theta)$. After applying the transform on center profile, a two-dimensional radon map is obtained as shown in Fig.6.

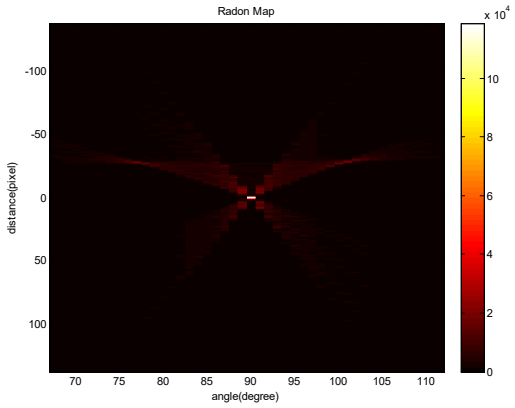

Fig. 6 Two-dimensional radon map.

By applying a local maxima algorithm on the Radon map, position and orientation of the longest straight line in the center profile image is detected. Thus, the main line is extracted from the image which is marked by the red line in Fig.7.

2) Edge Points Detection: In the center profile of laser stripe, the inflection points at both edges of welding joint is defined as edge points. The position of edge points could mark the location of weld seam for further feature extraction. The method of edge points detection is as follows. According to the property of Radon transform, the main line passes through more laser stripe pixels than other lines. Let U be the point set of center profile points in the region of welding joint. Hence for center profile point $C(j)$ not included in U, the necessary condition is

$$E_a(j)<M(j)<E_b(j)\quad (C(j)\notin U). \tag{16}$$

where $E_a(j)$ and $E_b(j)$ are the upper and lower boundary points of the laser stripe in j-th column and $M(j)$ is the points on the main line in j-th column. Now apply (16) to this condition, it is concluded that for $C(j)$ belongs to U, the sufficient condition is

$$\left|C(j)-M(j)\right|>\frac{1}{2}\left|E_a(j)-E_b(j)\right|\quad (C(j)\in U). \tag{17}$$

Using (17), the point set U could be calculated and all the points in U are located in welding joint area. Supposing that the smallest index j in set U is a and the largest is b, the leftmost point $C(a)$ and rightmost point $C(b)$ in the set U are determined as edge points. This method guarantees that occasional offset point in center profile would not be detected as edge point. The detection results are shown in Fig.7.

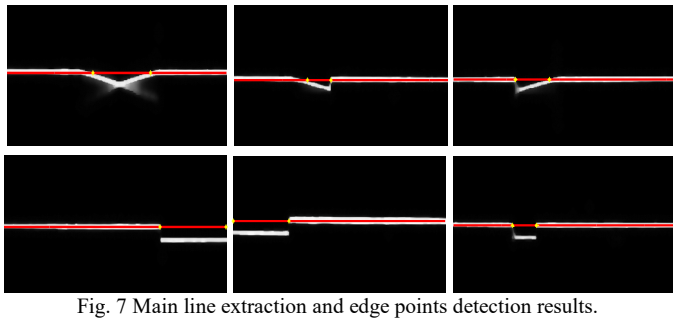

Fig. 7 Main line extraction and edge points detection results.

3) Feature Vector Computation: Provided that edge points $C(a)$ and $C(b)$ are extracted as shown in Fig.7, the feature vector is computed as follows. Firstly, the point $C(m)$ with largest deviation from the main line is selected.

$$m=\arg\max_j\left|C(j)-M(j)\right|\quad (C(j)\in U) \tag{18}$$

If there are several largest values, the median value of m is chosen as m. Noticing that there might be a small angle θ between the main line and the horizontal axis as shown in Fig.8, the column indexes of seven feature points are determined using (19), (20)

$$j=a+\frac{(k-1)(m-a)}{3},\quad (k=1,2,3,4) \tag{19}$$

$$j=m+\frac{(k-4)(b-m)}{3},\quad (k=5,6,7) \tag{20}$$

$$h(k)=\frac{C(j)-M(j)}{\cos\theta},\quad (k=1,2,...,7) \tag{21}$$

where j is the index of center profile point in j-th column. $h(k)$ is the distance between each feature point and the main line.

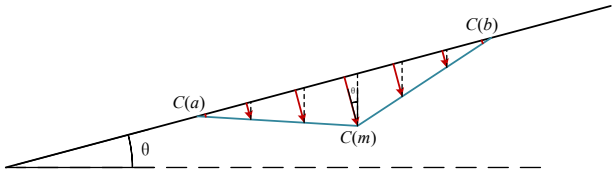

Fig. 8 Feature vector extraction.

Then the distance is normalized in order to reduce the influence of large value data.

$$\bar{h}(k)=\frac{h(k)}{\max\left|h(k)\right|},\quad (k=1,2,...,7) \tag{22}$$

Since the distance value could be identical for left and right lap joint grooves, noticing that the edge points of lap

joint are different from other joints, the feature values are designed as follows.

$$v(i) = \overline{h}(i-1), \quad (i = 2,3,...,8) \tag{23}$$

$$v(1) = \begin{cases} 1, & \text{if } a = 1 \\ 0, & \text{else} \end{cases} \tag{24}$$

$$v(9) = \begin{cases} 1, & \text{if } b = w \\ 0, & \text{else} \end{cases} \tag{25}$$

Thus the nine feature values are computed. For structured-light images of six different weld seam types, the feature vector of each image is expressed as follows

$$V = [v(1), v(2), ..., v(9)] \tag{26}$$

IV. Establishment of Classification Model

A. Ensemble Learning Methods

In supervised learning algorithms, the classification accuracy may be influenced by factors such as limited training samples. In order to improve the overall accuracy of classification model, the structure of ensemble learning model in weld seam recognition is shown in Fig.9. This model assembles several weak classifiers to produce a strong classifier. If some of the weak classifiers produce inaccurate results, the model may adjust the weight of training samples and classifiers accordingly and combines all the classifiers to produce a better result overall.

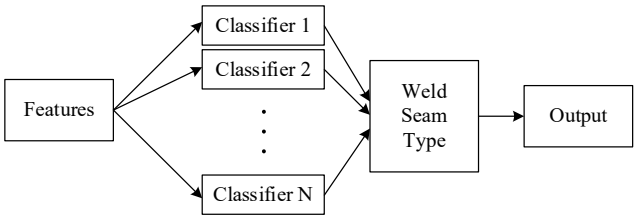

Fig. 9 Flow chart of ensemble learning methods.

B. BP-Adaboost Model

In BP-Adaboost model, BP neural network (BPNN) [14] is adopted as weak classifier and Adaboost algorithm is used as ensemble algorithm to combine weak classifiers. The input of classifiers is the feature and label of every image. The label vector is a 6-bit array where the bit corresponds to the class of weld seam is 1 and others are 0. The algorithm of Adaboost algorithm is presented below.

TABLE I
ADABOOST ALGORITHM FOR CLASSIFICATION

Input: training sample $(X,Y)=(x_i,y_i)$, i=1,2,…,N, where X is feature vector and Y is label vector.
Output: classification accuracy
1 Initialize weight distribution of sample $w_i=1/N$
2 **for** t=1,2,…,T **do**
3 train weak classifier with sample and get a prediction $H_t(X)$
4 calculate the error rate $e_t = \sum_1^N w_i(H_t(x_i) \neq y_i)$
5 calculate the weight of the weak classifier $\alpha_t = \ln((1-e_t)/e_t)/2$
6 update the weight of sample
if $H(x_i)=y_i$ **then**
$w_i = w_i/(2-2e_t)$
else
$w_i = w_i/(2e_t)$
end if
7 **end for**
8 calculate the strong classifier output $H_{final} = \sum_1^T \alpha_t H_t(X)$
9 normalize the output and compute classification accuracy

As the weak classifier, BPNN composes of three layers. There were nine nodes in the input layer, nine nodes in the hidden layer and six nodes in the output layer. The transfer function of input and hidden layer is sigmoid function, while linear function is used in the output node. Gradient descent method is adopted in training. This BPNN structure is suitable for multi-class classification task of six weld seam types.

C. KNN-Adaboost Model

In KNN-Adaboost model, K-Nearest Neighbour (KNN) method [15] is adopted as weak classifier. The algorithm of Adaboost and the input of classifier is the same as previous model.

For the weak classifier KNN, Euclidean distance is utilized to measure the distance between two samples. The sample point closest to the test sample point is chosen as the nearest neighbour, which means K equals to 1. KNN is a natural method for multi-class classification, so its structure is simple in this case.

V. Experiments and Results

Experiments on recognizing six weld seam types were conducted to verify the effectiveness of proposed recognition system showed in Fig.10.

Fig.10 Experiment configuration of proposed system.

The structured light vision sensor scanned the weld seam and captured 570 images of six types of weld seam. The images were divided into training set and testing set. To testify the robustness of proposed method, noises such as Gaussian noise, speckle noise and salt-and-pepper noise with various intensity were added to the testing set. In Fig.12 and Fig.13, if the intensity value is 1, the standard deviation of Gaussian noise and speckle noise is 0.2 and 0.4 respectively and the density of salt and pepper noise is 0.004. The noise intensity value is the multiple of the given deviation and density. Taking symmetric V groove for instance, the visualized result of proposed image processing and feature computation procedure with the noise intensity of 5 is presented in Fig.11. Moreover, the parameters in the feature extraction procedure were as follows: α=0.2,

β_1=2, β_2=1 and Δy =50 pixels. Therefore, several weld seam recognition experiments were carried out.

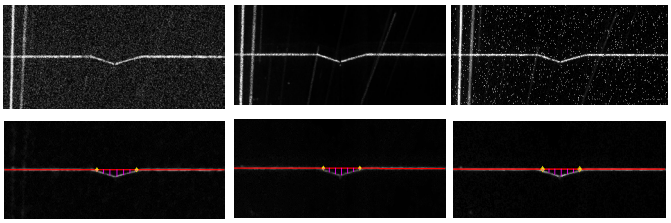

Fig.11 Results of feature computation under different noises.

The Fig.12 and Fig.13 showed the classification performance of the experiment. In Fig.12, the effectiveness of different classification algorithms is shown. The result is entirely accurate with minor noises. As can be seen in the line chart, ensemble learning method such as KNN-Adaboost and BP-Adaboost is more accurate than KNN and BPNN when severe noises exist. This is because the KNN and BPNN may suffer from one-time occasionality in the training process under the condition when training data are limited.

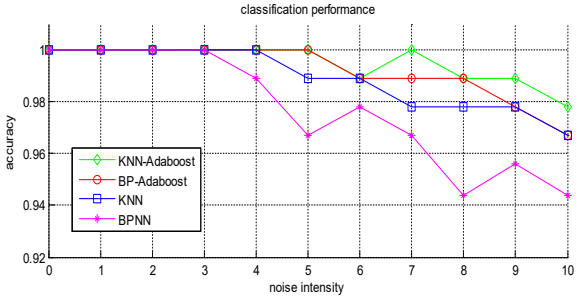

Fig.12 Performance of different classification algorithms.

In order to verify the robustness of proposed image process and feature extraction method. Proposed method was compared with the traditional weld seam feature computation method in [10]. The feature vectors of testing set using both methods were classified by KNN-Adaboost classifier. As is shown in Fig.13, compared to traditional method, proposed method is capable of extracting weld seam feature more accurately with the interference of noises.

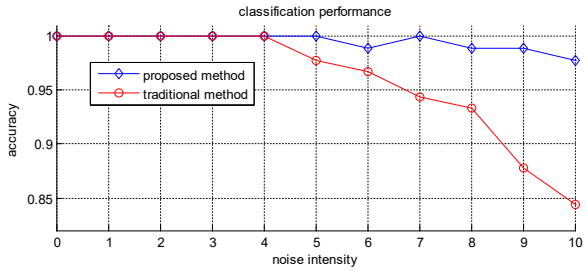

Fig.13 Performance of different feature extraction methods.

To sum up, the experiment result shows that the proposed feature extraction and classification method is robust and effective and the proposed system can be applied in harsh environment.

VI. Conclusion

As described in this paper, a weld seam type recognition system based on structured light vision and ensemble learning is developed. The noises from welding process are filtered out by optical filter and proposed image filtering method. The proposed laser stripe extraction and feature vector computation method can accurately extract essential features of six weld seam types. The proposed ensemble learning classification model is able to recognize the weld seam type precisely even in the presence of severe noises. In conclusion, the performance of proposed system is robust and effective. In the further research, the proposed system could be combined with seam tracking system to achieve automatic selection of welding parameters.

References

[1] J. Muhammad, H. Altun and E. Abo-Serie, "Welding Seam Profiling Techniques Based on Active Vision Sensing for Intelligent Robotic Welding," *The International Journal of Advanced Manufacturing Technology*, vol. 88, no. 1-4, pp. 127-145, 2017.

[2] J. Jia, H. Zhang and Z. Xiong, "A Fuzzy Tracking Control System for Arc Welding Robot Based on Rotating Arc Sensor," *2006 IEEE International Conference on Information Acquisition*, Shandong, 2006, pp. 967-971.

[3] T. F. Bastos, J. M. Martin, L. Calderon and R. Ceres, "Weld Seams Detection and Recognition for Robotic Arc-welding Through Ultrasonic Sensors," *Industrial Electronics, 1994. Symposium Proceedings, ISIE '94., 1994 IEEE International Symposium on*, Santiago, 1994, pp. 310-315.

[4] E. L. Estochen, C. P. Neuman and F. B. Prinz, "Application of Acoustic Sensors to Robotic Seam Tracking," in *IEEE Transactions on Industrial Electronics*, vol. IE-31, no. 3, pp. 219-224, Aug. 1984.

[5] Z. Fang, D. Xu and M. Tan. "Visual Seam Tracking System for Butt Weld of Thin Plate," *International Journal of Advanced Manufacturing Technology*, vol. 49, no. 5-8, pp. 519-526, 2010.

[6] Linkun Wang, De Xu and Min Tan, "Robust Detection for the Weld Seam Shaped Zigzag Line," *2004 IEEE International Conference on Robotics and Biomimetics*, Shenyang, 2004, pp. 721-726.

[7] L. Yang, E. Li, T. Long, J. Fan, Y. Mao and Z. Fang, et al. "A Welding Quality Detection Method for Arc Welding Robot Based on 3D Reconstruction with SFS Algorithm." *International Journal of Advanced Manufacturing Technology*, vol. 94, no. 1-4, pp. 1209-1220, 2018.

[8] J. Fan, F. Jing, Z. Fang and Z. Liang, "A Simple Calibration Method of Structured Light Plane Parameters for Welding Robots," *2016 35th Chinese Control Conference (CCC)*, Chengdu, 2016, pp. 6127-6132.

[9] X. Wang, X. Fan, Y. Fan and R. Bai, "Recognition of the Type of Welding Joint Based on Line Structured-light Vision," *The 27th Chinese Control and Decision Conference (2015 CCDC)*, Qingdao, 2015, pp. 4383-4386.

[10] J. Fan, F. Jing, Z. Fang and M. Tan, "Automatic Recognition System of Welding Seam Type Based on SVM Method," *International Journal of Advanced Manufacturing Technology,* vol. 92, no. 1-4, pp. 989-999, 2017.

[11] C. Cortes and V. Vapnik, "Support-vector Networks," *Machine Learning,* vol. 20, no. 3, pp. 273-297, 1995.

[12] F. Huang, G. Xie and R. Xiao, "Research on Ensemble Learning," *2009 International Conference on Artificial Intelligence and Computational Intelligence*, Shanghai, 2009, pp. 249-252.

[13] P. Perona and J. Malik, "Scale-space and Edge Detection Using Anisotropic Diffusion," in *IEEE Transactions on Pattern Analysis and Machine Intelligence*, vol. 12, no. 7, pp. 629-639, Jul 1990.

[14] D. Rumerlhart, G. Hinton and R. Williams, "Learning Representation by Back-propagating Errors," *Nature*, vol. 323, no. 3, pp. 533-536, 1986.

[15] T. Cover and P. Hart, "Nearest Neighbor Pattern Classification," in *IEEE Transactions on Information Theory*, vol. 13, no. 1, pp. 21-27, January 1967.